Lack of Pericytes Leads to Endothelial Hyperplasia and Abnormal Vascular Morphogenesis

Mats Hellström,*‡ Holger Gerhardt,*§ Mattias Kalén,* Xuri Li,‡ Ulf Eriksson,‡ Hartwig Wolburg,§ and Christer Betsholtz*

*Department of Medical Biochemistry, Göteborg University, SE-405 30 Göteborg, Sweden; ‡Ludwig Institute for Cancer Research, Stockholm Branch, Karolinska Institute, SE-171 77 Stockholm, Sweden; and §Institute of Pathology, University of Tuebingen, 72076 Tuebingen, Germany

Abstract. The association of pericytes (PCs) to newly formed blood vessels has been suggested to regulate endothelial cell (EC) proliferation, survival, migration, differentiation, and vascular branching. Here, we addressed these issues using PDGF-B– and PDGF receptor-β (PDGFR-β)–deficient mice as in vivo models of brain angiogenesis in the absence of PCs. Quantitative morphological analysis showed that these mutants have normal microvessel density, length, and number of branch points. However, absence of PCs correlates with endothelial hyperplasia, increased capillary diameter, abnormal EC shape and ultrastructure, changed cellular distribution of certain junctional proteins, and morphological signs of increased transendothelial permeability. Brain endothelial hyperplasia was observed already at embryonic day (E) 11.5 and persisted throughout development. From E 13.5, vascular endothelial growth factor-A (VEGF-A) and other genes responsive to metabolic stress became upregulated, suggesting that the abnormal microvessel architecture has systemic metabolic consequences. VEGF-A upregulation correlated temporally with the occurrence of vascular abnormalities in the placenta and dilation of the heart. Thus, although PC deficiency appears to have direct effects on EC number before E 13.5, the subsequent increased VEGF-A levels may further abrogate microvessel architecture, promote vascular permeability, and contribute to formation of the edematous phenotype observed in late gestation PDGF-B and PDGFR-β knock out embryos.

Key words: mice • angiogenesis • pericytes • platelet-derived growth factor B • vascular endothelial growth factor

Introduction

The vascular system is the first functional organ in the developing vertebrate embryo and its continuous growth is required for embryonic development. The first blood vessels develop from mesenchymal cells that differentiate into endothelial tubes and interconnect to form a primitive blood vessel network. New blood vessels develop from this vascular plexus by angiogenesis, which comprises endothelial sprouting, splitting, and fusion (Risau, 1997). Soon after the first endothelial tubes have formed, they become associated with mural cells of the smooth muscle cell lineage, referred to as pericytes (PCs)[1] or vascular smooth muscle cells (vSMCs) (Sims, 1986).

The PC/vSMCs are probably induced de novo from the mesenchyme surrounding the endothelium (Beck and D'Amore, 1997). In vitro experiments implicate TGF-β in this process (Antonelli-Orlidge et al., 1989; Sato and Rifkin, 1989; Hirschi et al., 1998). In addition, targeted mutagenesis in mice implicates TGF-β signaling in the process of PC/vSMC development (Li et al., 1999; Yang et al., 1999; Oh et al., 2000). An early role for angiopoietin-1 and its receptor Tie-2 in the formation of PC/vSMCs is suggested from the phenotypes of angiopoietin-1 and Tie-2 knock outs, which both exhibit reduced embryonic PC/vSMC formation (Suri et al., 1996; Patan, 1998). In addition, humans with a point mutation in the *tie-2* gene activating its tyrosine kinase exhibit venous malformations with regionally reduced vSMC coating (Vikkula et al., 1996).

After induction, the population of PC/vSMCs is expanded and recruited to angiogenic sprouts by means of proliferation and migration (Nicosia and Villaschi, 1995;

Address correspondence to Christer Betsholtz, Department of Medical Biochemistry, Göteborg University, P.O. Box 440, SE-405 30 Göteborg, Sweden. Tel.: 46-31-7733460. Fax: 46-31-416108. E-mail: christer.betsholtz@medkem.gu.se

[1]*Abbreviations used in this paper:* E, embryonic day; EC, endothelial cell; Glut-1, glucose transporter 1; LDH, lactate dehydrogynase; PC, pericyte; PDGFR-β, PDGF receptor-β; PGK, phosphoglycerate kinase; VEGF-A, vascular endothelial growth factor-A; vSMC, vascular smooth muscle cell.

Beck and D'Amore, 1997; Benjamin et al., 1998). This longitudinal spreading of PC/vSMCs along growing blood vessels depends on PDGF-B and PDGF receptor-β (PDGFR-β) (Lindahl et al., 1997; Hellstrom et al., 1999). In the developing mouse embryo, PDGF-B is produced by the endothelium, whereas PDGFR-β is expressed by developing PC/vSMCs (Holmgren et al., 1991; Lindahl et al., 1997). Targeted disruption of PDGF-B or PDGFR-β genes both lead to formation of blood vessels lacking PC/vSMCs. Chimeric analysis of wild-type and PDGFR-β–null cells has shown that PDGFR-β is cell autonomously required in the PC/vSMC lineage (Crosby et al., 1998; Lindahl et al., 1998). Together, these data suggest that longitudinal recruitment of PC/vSMCs is controlled by paracrine signaling involving PDGF-B released from endothelial cells (ECs) to act on PDGFR-β expressed by neighboring PC/vSMCs.

The PDGF-B– and PDGFR-β–null mutations are homozygously lethal at birth. The immediate cause of lethality appears to be a sudden onset of microvascular hemorrhaging and edema formation. However, multiple cardiovascular abnormalities are apparent from earlier embryonic age, including cardiac dilation and hypertrabeculation, abnormal kidney glomeruli lacking mesangial cells, an abnormal placenta labyrinthine layer, and dilation of large and small caliber blood vessels (Levéen et al., 1994; Soriano, 1994; Lindahl et al., 1997; Hellstrom et al., 1999; Ohlsson et al., 1999). The microvascular hemorrhaging is preceded by the formation of microaneurysms, which are morphologically similar to the characteristic lesions in human diabetic microangiopathy (Cogan et al., 1961). It is possible that all phenotypes observed in PDGF-B and PDGFR-β knock outs are caused by a reduction in the abundance of PC/vSMCs, but both the normal role of PCs in microvessels and the pathogenesis of the cardiovascular changes in PDGF-B and PDGFR-β knock outs remain unclear. It is likely, however, that PCs influence EC behavior. PCs have been suggested to have a role in endothelial sprouting, and the localization of PCs to capillary branch points suggests a role in vascular branching morphogenesis (Nehls et al., 1994). It has been proposed that PCs negatively regulate EC proliferation in vitro (Orlidge and D'Amore, 1987; Hirschi et al., 1999). On the other hand, PCs appear to promote EC survival in the pruning process during formation of the retinal vasculature and in tumor vessels after experimental withdrawal of the vascular endothelial growth factor-A (VEGF-A) (Benjamin et al., 1998, 1999). Based on these findings, the lack of PCs in vivo would either be predicted to lead to an increase in EC proliferation, resulting in EC hyperplasia, or to a decreased EC survival, resulting in EC hypoplasia. Although mechanistically conflicting, both results could lead to vascular dysfunction and cause the phenotypes observed in PDGF-B– and PDGFR-β–null embryos. The present investigation addresses the role of PCs making use of the unique properties of PDGF-B– and PDGFR-β–deficient mice as an in vivo model of brain angiogenesis in the absence of PCs (Lindahl et al., 1997; Hellstrom et al., 1999). We show that PCs are not determining microvessel density, length, or branching, but are involved in the regulation of EC number and morphology and microvessel architecture.

Materials and Methods

Animals

Mice harboring the deletion of the PDGF-B and PRDGFR-β genes were bred as heterozygous outbred hybrids of 129/sv and C57Bl6 (Levéen et al., 1994; Soriano, 1994). Ages of embryos subject to analysis were given as embryonic day (E) where the vaginal plug was scored on E 0.5 and birth usually took place on E 19. The indicated number of embryos of the different genotypes (wild type, PDGF-B knock outs, PDGFR-β knock outs) were used for each type of analysis below. EC quantification: E 10.5 (2, 2, 2), E 11.5 (5, 3, 2), E 12.5 (2, 2, 0), E 14.5 (2, 2, 0), E 16.5 (2, 3, 0), E 18.5 (2, 2, 2). Capillary morphometry: E 17.5 (2, 0, 2). Immunohistochemistry: E 18.5 (2, 2, 2), E 12.5 (2, 2, 2). Electron microscopy: E 18.5 (3, 4, 0). VEGFA measurements (figures indicate number of samples analyzed from head or brain/liver): E 12.5 (4/3, 5/2, 2/0), E 13.5 (4/10, 2/5, 2/5), E 14.5 (3/3, 3/3, 1/1), E 16.5 (3/2, 3/3, 3/2), E 18.5 (3/2, 4/4, 4/4). RNA analysis: E 17.5 (3, 0, 3).

EC Quantification and Capillary Morphometry

Capillary EC nuclei were counted on 5-μm paraffin sections of brains fixed in 4% paraformaldehyde. Sections were stained with propidium iodide and biotinylated isolectin BS-I (L-2140; Sigma-Aldrich) as described (Hellstrom et al., 1999), except for the use of streptavidin Alexa 488 (S-11223; Molecular Probes) at a final concentration of 2 μg/ml. EC nuclei were counted using the 60× objective on a Nikon Eclipse E1000 microscope with a fluorescent filter allowing simultaneous monitoring of red and green signals. For morphometric analysis, 14-μm sections were stained with isolectin BS-I and horseradish peroxidase (Hellstrom et al., 1999) and analyzed using the 10× objective on an Optronics charge-coupled device camera and associated software. Capillary blood vessel length and branching were quantified on 15 photographic areas. The capillary diameter was quantified on 15 photographic areas at 200 sites.

Immunohistochemistry

The following antibodies were used at the dilutions indicated: polyclonal rabbit anticaveolin-1 (1:500; Transduction Laboratories), polyclonal rabbit antiaquaporin-4 (1:100; Chemicon), polyclonal rabbit anticlaudin-1 (1:500; Zymed), polyclonal rabbit antioccludin (1:200, clone Z-T22; Zymed), polyclonal rabbit anti–ZO-1 (1:500; Zymed), rat monoclonal anti–VE-cadherin (culture supernatant; provided by Dr. Dietmar Vestweber, University of Muenster, Muenster, Germany), FITC-conjugated polyclonal sheep antifibronectin (1:100; Biotrend), polyclonal rabbit anticlaudin-5 (1:1,000; production described in Liebner et al., 2000). Embryonic brains were dissected and directly frozen in Tissue-Tek OCT (Miles Scientific). Cryosections were cut at 12 μm, mounted on glass slides, air dried, and fixed in ice-cold ethanol for 5 min followed by 1 min in acetone at room temperature. Sections were rinsed and incubated with the primary and appropriate secondary antibodies as described (Gerhardt et al., 1996). Slides were coverslipped using Moviol and analyzed using a Leica TCS NT confocal laser scanning microscope (Leica). For direct comparison between wild-type and knock out brains, sections were mounted pairwise on the slides. Photomultiplier settings were identical for image acquisition from knock out and wild-type specimen.

Electron Microscopy

Embryos were fixed by perfusion through the heart of 2.5% glutaraldehyde in Hank's modified salt solution buffer. Brains were immersion fixed in the same fixative for an additional 4 h, washed, postfixed, dehydrated, and processed for transmission electron microscopy as described (Gerhardt et al., 1996). For freeze fracture analysis, tissue specimens were fixed as above, cryoprotected for freeze fracture in 30% glycerol, and frozen in nitrogen slush (−210°C). Subsequent freeze fracture of the tissue and analysis by electron microscopy was done as described (Kniesel et al., 1996).

RNA Analyses

Total RNA was prepared from snap frozen brain tissue using the RNeasy midi kit (75144; QIAGEN) according to the manufacturer's protocol. For Northern blot analysis, 10 μg RNA was used for Northern blot analysis by the NorthernMax Kit (1940; Ambion). Mouse probes for β-actin, GRP-78, and glucose transporter 1 (Glut-1) and rat probes for phosphoglycerate kinase (PGK) and lactate dehydrogynase (LDH; probes provided by Dr.

Peter Carmeliet, Center for Transgene Technology and Gene Therapy, Leuven, Belgium) were randomly labeled using Megaprime DNA labeling system (RPN 1607; Amersham Pharmacia Biotech) according to the manufacturer's protocols. For RNase Protection analysis, 30 μg of RNA was used in the RPA III kit (1414; Ambion), and polyacrylamide gels were exposed and scanned using a BAS-1500 PhosphoImager (Fuji). Riboprobes were prepared using RNA polymerase (Promega) and [^{32}P]UTP (Amersham Pharmacia Biotech) according to the manufacturer's protocol. Mouse cDNA fragments used as templates to make the probes are as follows: Flt-1, 437 bp, NM_002019.1; Tie1, EcoRI fragment of ~400 bp, X80764; Flk-1, 725 bp, X70842. β-Actin template (Ambion), which generates a 250-bp protected fragment, was used as an internal control for quantification.

VEGF-A Measurements

Tissues were snap frozen and kept at −80°C until analysis and subsequently lysed and homogenized in 150 mM NaCl, 66 mM EDTA, 10 mM Tris-HCL (pH 7.4), 0,4% sodiumdeoxycholate, 1% NP-40, and protease inhibitor cocktail (P-2714; Sigma-Aldrich). The VEGF-A ELISA detection kit (MMV00; R&D Systems) was used to quantify VEGF-A protein from tissue lysates. The plates were read in a Kinetic microplate reader (Molecular Devices). The VEGF-A concentration was normalized against the total amount of protein in the sample using protein assay (500-0006; Bio-Rad Laboratories).

Statistics and Image Processing

The two-tailed paired Student's *t* test was used for all statistical calculation. Pictures were assembled and processed in Adobe® Photoshop™, v5.5.

Results

EC Hyperplasia in PDGF-B– and PDGFR-β–deficient Embryos Correlates with Lack of PCs in the Brain

We compared the number of ECs in the brains of wild-type and PDGF-B and PDGFR-β knock out embryos by counting the number of EC nuclei per capillary cross section (Fig. 1). The number of nuclei per cross section varied throughout development and was higher at the earlier time points (Fig. 1 b). There was an increase of ~60% in the number of nuclei per capillary cross section in PDGF-B and PDGFR-β knock out brains from E 11.5 on (Fig. 1 c). This increase persisted throughout prenatal development and correlated with the lack of PCs in the PDGF-B and PDGFR-β knock out brains seen at E 11.5 and throughout prenatal development (Hellstrom et al., 1999; data not shown). Studies of longitudinally sectioned capillaries and serial sections showed that EC nuclear shape was not altered in mutants (not shown). Thus, an increased nuclear count reflects EC hyperplasia. EC hyperplasia was not observed in the perineural vascular plexus surrounding the brain (data not shown) where PCs are still present in the PDGF-B and PDGFR-β knock out embryos (Lindahl et al., 1997; Hellstrom et al., 1999). BrdU and TdT-mediated dUTP-biotin nick end labeling staining was analyzed at several time points between E 10.5 and E 18.5, but no significant differences between wild-type and mutant embryos were revealed (data not shown). This excludes a simultaneous large increase in proliferation and apoptosis, but the sensitivity of the analysis does not allow small changes in cell number that may arise over several cell cycles to be correctly determined.

To assess if the density and branching of vessels was affected by PC absence, morphometric analysis was done of closely matched photographic areas of E 17.5 brains from

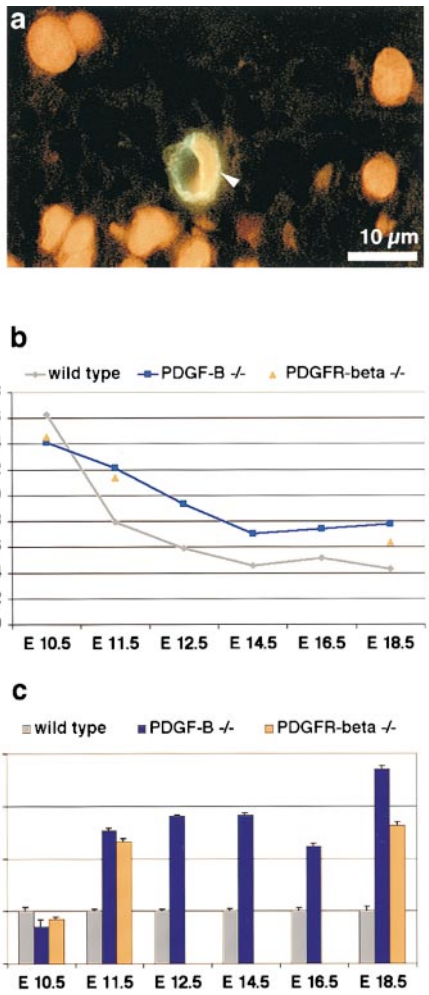

Figure 1. EC quantification in wild type, PDGF-B, and PDGFR-β knock out embryos. A brain capillary stained for isolectin BS-I (staining EC, green) and propidium iodide (staining nuclei, red) (a). The quantification of EC nuclei per vessel cross section in wild type, PDGF-B$^{-/-}$, and PDFGFR-β$^{-/-}$ is shown in b, and the values for the mutants are shown as a percentage of the wild type in c. There is a prominent EC hyperplasia from E 11.5 on in the PDGF-B and PDGFR-β knock outs. The error bars represent the SEM. PDGF-B and PDGFR-β knock out values were significantly different (p-value < 0.001) from the wild-type values at E 11.5, 12.5, 13.5, 14.5, 16.5, and 18.5, but not at E 10.5. Bar, 10 μm.

wild-type and PDGFR-β knock out embryos. There were no significant changes in average total blood vessel length (1.133 ± 21 μm [SEM] per photographic area for wild type and 1.118 ± 23 μm for PDGFR-β knock out). Also, the numbers of blood vessel branch points were similar in wild type and PDGFR-β knock out (6.3 ± 0.22 [SEM] per photographic area for wild type and 5.6 ± 0.25 branch points for PDGFR-β knock out).

We performed RNase Protection assays for the endothelial receptor tyrosine kinases VEGFR-1/Flt-1, VEGFR-2/Flk-1, and Tie1 to assess if these transcripts were altered in the mutants. Total RNA was analyzed at E 17.5 in the wild-type and PDGFR-β knock out brains and normalized against β-actin. In the PDGFR-β knock out brain, the VEGFR-1 signal was 146% compared with wild type (p-value = 0.077), VEGFR-2 signal was 179% compared with

wild type (p-value = 0.002), and Tie1 signal was 259% compared with wild type (p-value = 0.02). There is good correlation between the magnitudes of the expression of VEGFR-1 and -2 and the EC hyperplasia, suggesting that the expression of VEGFR-1 and -2 is not altered in the absence of PCs. The larger increase in Tie1 compared with VEGFR-1 and -2 expression in mutants is compatible with a previous report that Tie1-driven LacZ expression is increased in the PDGF-B knock out (Lindahl et al., 1997).

Abnormal Blood Vessel Morphogenesis in PDGF-B and PDGFR-β Knock Outs

The EC hyperplasia prompted us to assess vessel diameter and EC–EC interaction. The mean blood vessel diameter was increased by 25% ($P < 0.001$) in the PDGFR-β knock out compared with wild type but was highly variable (Fig. 2 a). The blood vessels of the PDGF-B and PDGFR-β knock outs exhibited regional dilations along the blood vessel length, which was not seen in the wild type. (Fig 2, b and c; data not shown).

We used the tight junction marker ZO-1 to measure the circumferential length of EC junctions at E 18.5, (Fig. 2, d and e), a measure relating to the vessel surface occupied by individual ECs. Vessel dilation without corresponding increase in the number of ECs would lead to a larger mean EC circumference. Circumferential length was, however, reduced by 25% ($P < 0.001$) in the PDGFR-β knock out, suggesting less expanded ECs or a greater overlap between ECs, or possibly a combination of both. Thus, in spite of vessel dilation in the knock outs, ECs were, on average, more densely packed in the capillary walls.

Increased Levels of VEGF-A in PDGF-B and PDGFR-β Knock Out Brains and Livers

We performed ELISA quantification of VEGF-A protein in brain and liver at several time points throughout development to determine its relation to EC hyperplasia in the PDGF-B and PDGFR-β knock out brains. The liver was added to the analysis since liver PCs are recruited independently of PDGF-B and PDGFR-β (Hellstrom et al., 1999). In PDGF-B and PDGFR-β knock outs, VEGF-A levels were progressively increased in both the brain and the liver from E 13.5 until birth (Fig. 3, a and b). By Northern blot analysis, the VEGF-A RNA level was also upregulated at E 16.5 in the PDGF-B knock out (data not shown).

Increased Expression of Genes Responsive to Metabolic Stress in PDGF-B Knock Out Brains

Since VEGF-A expression is influenced by metabolic stress such as hypoxia and hypoglycemia, we analyzed the relative levels of several other transcripts responsive to such stress: Glut-1, glucose-regulated protein 78, LDH, and PGK. Northern blot analysis revealed an approximately twofold upregulation of all these genes in PDGF-B knock out compared with wild-type and heterozygous E 16.5 brains (Fig. 4; data not shown). This indicates that the PDGF-B knock out embryos suffer from metabolic stress, which could be an important determinant of the increased VEGF-A expression in mutant embryos.

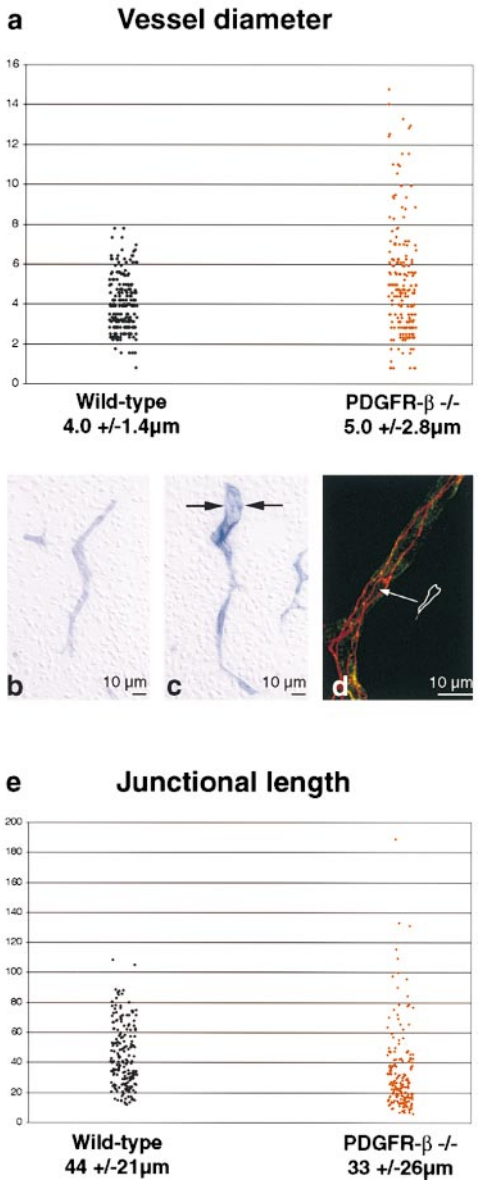

Figure 2. Vessel diameter and EC tight junction length in wild type and PDGFR-β knock out brains. Vessel diameter was measured on photographic areas from brain sections in wild type and PDGFR-β–deficient embryos at 200 locations each (a). The mean diameter was 4.0 ± 1.4 μm (SD) in the wild-type and 5.0 ± 2.8 μm in the PDGFR-β knock out embryos. There was a considerable variation of the diameter in the PDGFR-β knock out values (a), which was also seen at the microscopic level in a comparison between wild-type (b) and PDGF-B knock out (c) vessels. The vessels in the PDGF-B knock out embryos exhibited large differences in the vessel diameter with local severe dilations (arrows), whereas the wild-type vessels were more homogeneous in size. The circumferential length of 100 EC junctions (ZO-1 staining, red) were measured, as marked in d, in wild-type and PDGFR-β knock out vessels (e). The mean circumferential length was 44 ± 21 μm (SD) in the wild type and 33 ± μm 26 in the PDGFR-β knock out. Bar, 10 μm.

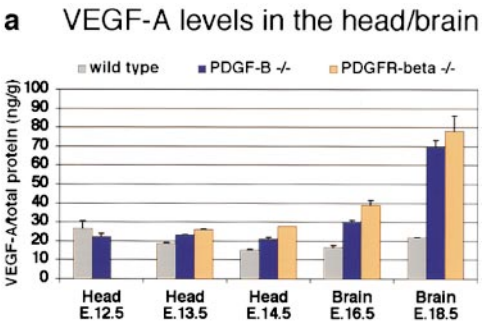

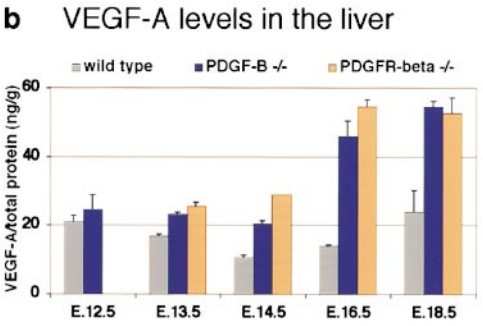

Figure 3. A time course of VEGF-A ELISA measurements. VEGF-A levels were upregulated from E 13.5 on in both PDGF-B and PDGFR-β knock out head/brain (a) and liver (b). The VEGF-A concentration was normalized against the total protein in the tissue sample. There were no significant differences between PDGF-B and PDGFR-β knock out values. The SEM is shown as error bars.

Abnormal Ultrastructural EC Morphology and Increased Caveolae Formation in PDGF-B and PDGFR-β Knock Out Brains

The morphological appearance of differentiated ECs is highly organized. The luminal surface is smooth, and the cytoplasmic thickness is uniform (Fig. 5, a and c). The ultrastructural analysis of PDGF-B knock out brain at E 17.5 revealed a highly abnormal EC morphology (Fig. 5, b and d). The luminal surface had multiple processes projecting into the lumen of the vessel (Fig. 5 d). In contrast to the wild type, the thickness of the knock out endothelium varied considerably (Fig. 5, b and d). In some areas, the cytoplasm of the cells was extremely thin, whereas at other sites it was considerably thicker than wild type. Another prominent feature of the PDGF-B knock out endothelium was the increase in the number of caveolae, which are vesicles involved in fluid and macromolecular transport across the endothelium (Figs. 5, e–h, and 6, a and b). Quantification revealed a 2.5-fold increase in the number of caveolae (counting caveolae per micrometer of vessel perimeter on electron micrographs at 30,000× magnification, 50 microvessels; data not shown). Consistent with an increase of fluid transport, many glia cells juxtaposed to the ECs of the PDGF-B knock out vessels exhibited prominent swelling, which was not seen in the wild type (Fig 6 d).

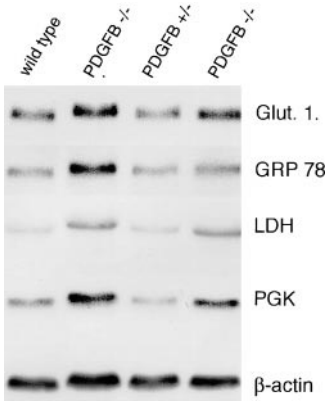

Figure 4. Northern blot analysis of mRNAs regulated by hypoxia, hypoglycemia, and metabolic stress. Brain total RNA from wild type, PDGF-$B^{+/-}$, and PDGF-$B^{-/-}$ were analyzed by Northern blot for Glut-1, glucose-regulated protein 78, LDH, and PGK. β-Actin was used as an internal control. The PDGF-B knock out brain showed upregulation of all these transcripts, especially LDH and PGK.

Increased Immunostaining for Caveolin-1 and Aquaporin-4 in PDGF-B and PDGFR-β Knock Out Brains

Caveolae in ECs are marked by the protein caveolin-1 (for review see Parton, 1996). Therefore, caveolin-1 immunostaining was carried out to determine whether the increased number of caveolae was also accompanied by corresponding increase in caveolin-1 labeling. Confocal laser scanning microscopy of PDGFR-β knock out brain endothelium showed an increased punctuate caveolin-1 staining (Fig. 6, a and b). However, in the highly permeable vessels of the choroid plexus, both the wild type and the PDGFR-β knock out exhibited equally high expression levels (Fig. 6, c and d). To assess if the glial swelling was accompanied by alterations in staining for water channel proteins, we immunolabeled aquaporin-4, which, in the brain, is specifically expressed by astrocytic cells. Aquaporin-4 revealed a heterogeneous staining but prominent upregulation in the immediate proximity of highly abnormal blood vessels in the PDGFR-β knock out (Fig. 6, e and f). Similar changes in caveolin-1 and aquaporin-4 expression were found in PDGF-B knock outs (data not shown).

Redistribution of VE-Cadherin and Occludin in ECs of PDGF-B and PDGFR-β Knock Out Brains

To further analyze the basis for vascular leakage in PDGF-B and PDGFR-β knock outs, we performed a detailed analysis of adherens and tight junction proteins by immunolabeling and confocal laser scanning microscopy. VE-cadherin, the major cadherin involved in EC–EC contact (Breier et al., 1996; Navarro et al., 1998), exhibited reduced junctional staining and increased cytoplasmic distribution in the PDGFR-β knock out compared with wild type at E 18.5 (Fig. 7, a and b), but no difference was seen at E 12.5 (data not shown). Occludin, an integral part of the tight junction (Furuse et al., 1993), showed less distinct junctional staining in PDGFR-β knock out ECs compared with wild type at E 18.5 (Fig. 7, d and e). This difference was not seen at E 12.5 (data not shown). Similar changes in cellular distribution of VE-cadherin and occludin were found in brain vessels of E 18.5 PDGF-B knock outs (data not shown). Analysis of the tight junction proteins ZO-1 and claudin-1 and -5 revealed no differences in junctional localization or staining intensity in PDGF-B or PDGFR-β knock outs at E 18.5 or E 12.5 (Fig. 7, g and h; data not

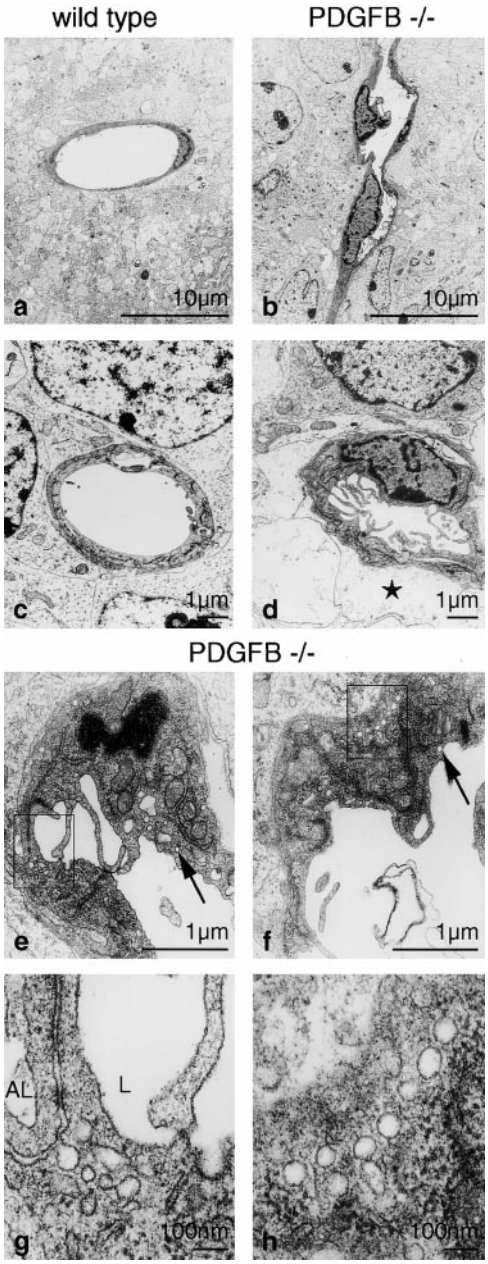

Figure 5. Electron micrographs of brain capillaries in wild-type (a and c) and PDGF-B knock out (b and d–h) embryos at E 18.5. Capillaries in wild-type embryonic brains exhibited a smooth luminal and abluminal endothelial surface and a homogenous thickness of the endothelium (a and c), whereas those in PDGF-B–deficient embryos were of highly variable thickness (b and d). Luminal microfolds greatly enlarged the endothelial surface (d), and perivascular glial swelling was prominent (star in d). Caveolae were abundant in the endothelium of knock out embryos (e–h), both near the luminal (arrows) and the abluminal surface (boxed area, enlarged in g and h). In g, a series of caveolae appeared almost to connect the luminal and the abluminal compartment. Bars: (a and b) 10 μm; (c–f) 1 μm; (g and h) 100 nm.

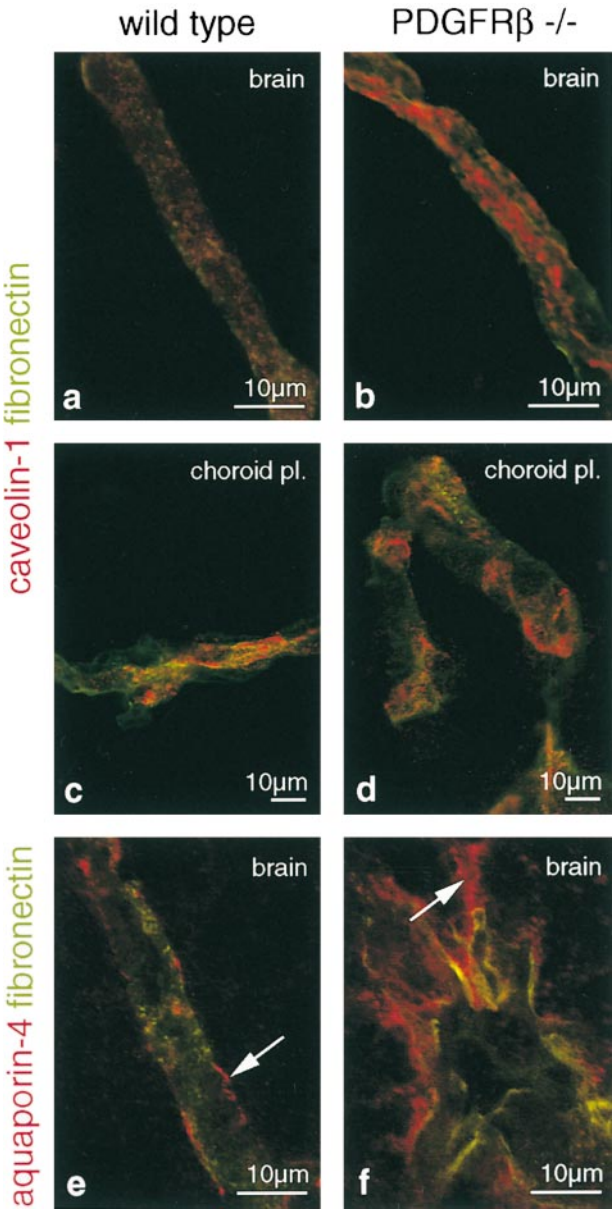

Figure 6. Confocal laser scanning micrographs of double immunolabeling for fibronectin (green) and caveolin-1 (a–d, red), and for fibronectin (green) and aquaporin-4 (e and f, red) at E 18.5. Caveolin-1 was considerably more abundant in brain capillaries of PDGFR-β knock out mice (compare a with b). The highly permeable endothelium of the choroid plexus was strongly immunopositive for caveolin-1 in both wild-type (c) and knock out embryos (d). In wild-type mice, aquaporin-4 labeling neatly outlined the blood vessels (e, arrow) whereas it was widely distributed into the surrounding brain parenchyma in knock out embryos (f, arrows). Bars, 10 μm.

shown). The microaneurysms typical for the PDGF-B and PDGFR-β knock out brains exhibited highly abnormal staining for all the above mentioned proteins (Fig. 7, c, f, and i), most likely coupled to the extreme endothelial morphology at these sites.

Alterations in the permeability of endothelial tight junctions correlate with characteristic morphological changes on freeze fracture images (for review see Kniesel and Wolburg, 2000). Upon cleavage of the two-cell membrane leaflets, the tight junctional particles remain inserted in either the external leaflet or in the protoplasmic leaflet, thus leaving a pit on the corresponding fracture face. The relative amount of p-face–associated tight junction particles

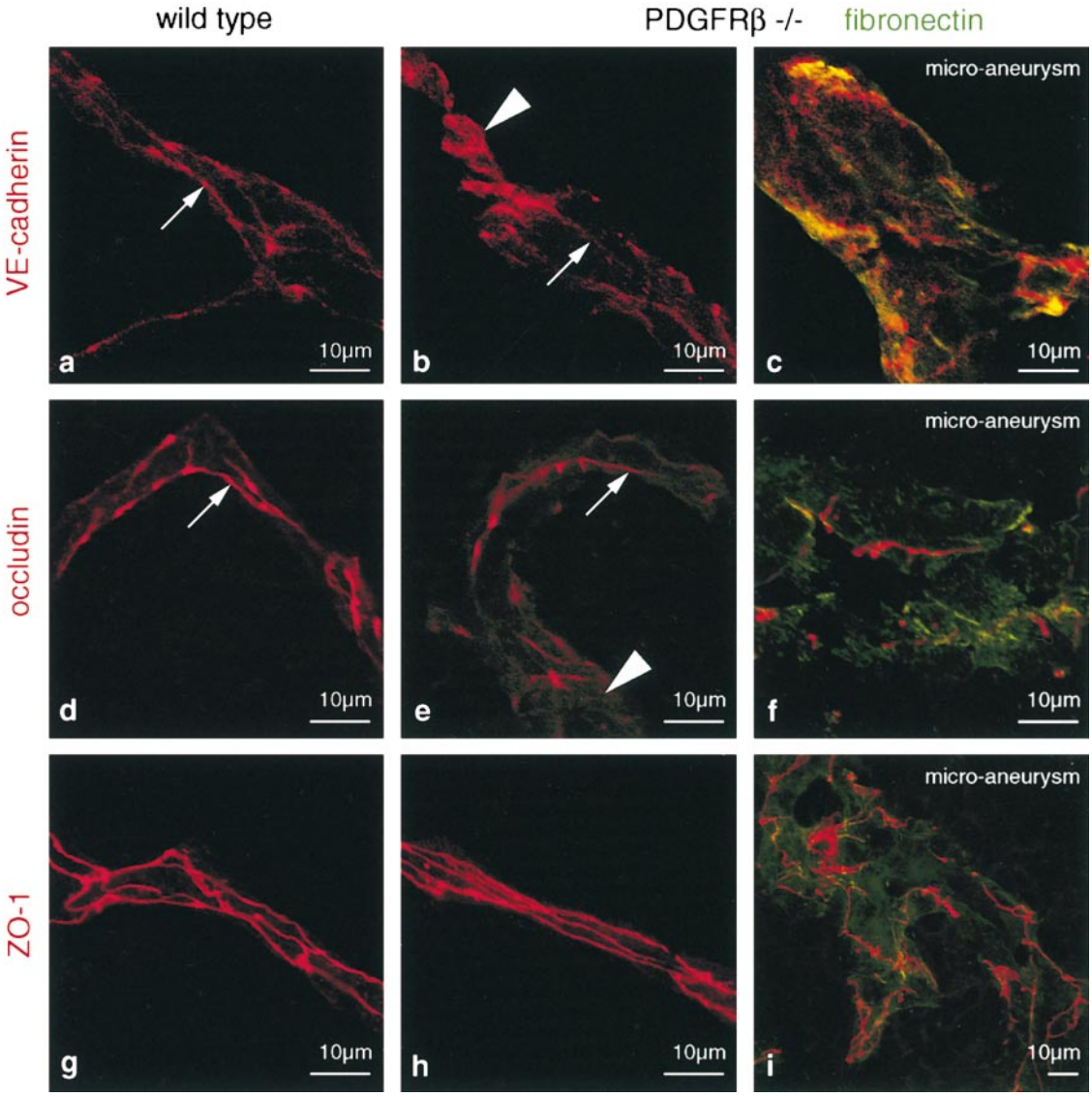

Figure 7. Confocal laser scanning micrographs of immunolabeling for VE-cadherin (a–c), occludin (d–f), and ZO-1 (g–i) at E 18.5. (Left) Wild type. (Middle and right) PDGFR-β knock out. (Right) Show examples of brain microaneurysms with additional fibronectin staining (green) to outline the vessels. In brain capillaries of wild type mice, VE-cadherin was largely confined to the interendothelial junction (a, arrows), whereas in those of knock out embryos, VE-cadherin was more uniformly distributed (b and c). Arrow indicates weak junctional labeling; arrowhead points to cytoplasmic labeling. Occludin labeling was also more diffuse in the knock out (compare d with e; arrow, junctional labeling; arrowhead, cytoplasmic labeling). In microaneurysms, the occludin-positive junctional network was discontinuous (f). ZO-1 was equally confined to the junction in both wild-type (g) and knock out mice (h). Differences in the pattern, as shown for a microaneurysm (i), reflect the highly irregular endothelial organization at this site. Bars, 10 μm.

reaches 55–60% in the mature mammalian blood–brain barrier but lies considerably lower during embryonic development (Kniesel et al., 1996). A second parameter of tight junction integrity is the complexity of the junctional network, reflecting the branching frequency of the tight junctional strands. Freeze fracture analysis was therefore performed on the tight junction of the vessels in the PDGF-B knock out at E 18.5 but did not reveal any apparent differences when compared with wild-type embryos (Fig. 8, a and b). For both wild-type and knock out embryos, the tight junctional appearance resembled that published for embryonic rat brain endothelium at E 18 (Kniesel et al., 1996).

Discussion

It has previously been shown that PDGF-B is produced by ECs and that PDGFR-β is present on PC/vSMCs (Holmgren et al., 1991; Lindahl et al., 1997; Hellstrom et al., 1999). PDGFR-β–negative cells fail to contribute to the PC/vSMCs lineage in mouse chimeras but contribute to the endothelium (Crosby et al., 1998; Lindahl et al., 1998). The endothelial phenotypes observed in PDGF-B and PDGFR-β knock outs are therefore most likely secondary to the lack of PCs along the vessels and may reflect deficient paracrine/juxtacrine PC-to-EC signaling or increased VEGF-A levels secondary to systemic metabolic stress caused by dysfunction of the cardiovascular system

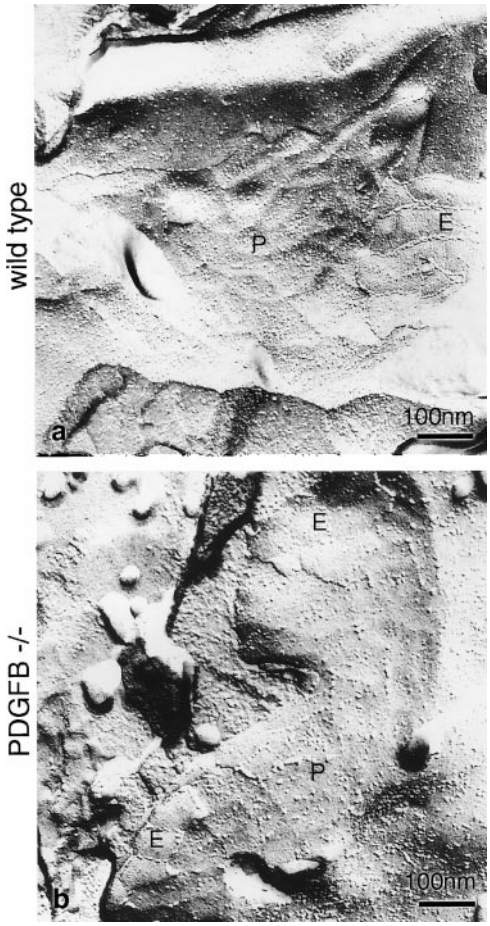

Figure 8. Freeze fracture replicas of brain capillary tight junctions of wild-type (a) and PDGF-B knock out (b) embryos at E 18.5. The tight junction particles were mostly associated to the external membrane leaflet (E) and only sparsely distributed on the protoplasmic membrane leaflet (P) in both the wild type and the knock out. The complexity of the junctional network as judged by the branching frequency of the strands was similar between wild type and PDGF-B knock out. Bars, 100 nm.

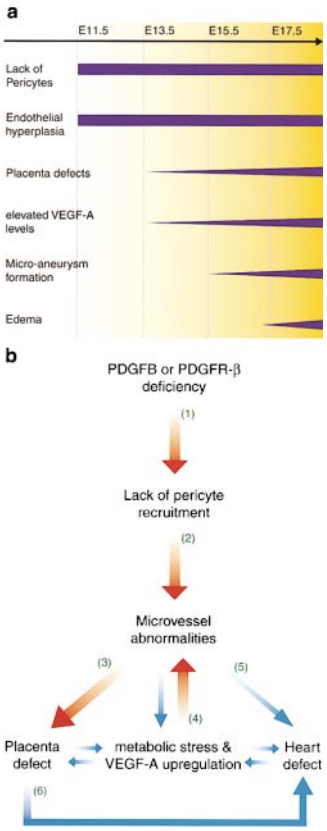

Figure 9. (a) Occurrence of phenotypes in the PDGF-B and PDGFR-β knock out embryos. The lack of PCs in PDGF-B and PDGFR-β knock out embryos coincides with the EC hyperplasia at E 11.5. At E 13.5, the first morphological signs of the placenta defects are evident, and this is also when an upregulation of VEGF-A is detected. Subsequently microaneurysms develop, and at late gestation, the embryos are edematous. (b) Hypothetical pathogenic cause–effect relationships in PDGF-B and PDGFR-β knock outs. Causal links supported by strong experimental evidence or extensive correlative data are depicted by thick red arrows. Causal links, which are plausible but lack or have only limited experimental support, are depicted with thin blue arrows. PDGF-B and PDGFR-β are required for the longitudinal recruitment of PCs to newly formed blood vessels, and lack of PCs leads to microvessel abnormalities (1 and 2) (Levéen et al., 1994; Soriano, 1994; Lindahl et al., 1997; Hellstrom et al., 1999; Ohlsson et al., 1999). Deficient blood vessel development in the placenta leads to improper placenta function (3) (Ohlsson et al., 1999; Ihle, 2000), which might promote hypoxia/hypoglycemia–induced VEGF-A, leading to microvessel abnormalities (4) (this report; Benjamin et al., 1998). The heart defect in the PDGF-B and PDGFR-β knock outs might stem from the abnormal heart vasculature or be due to placenta defects (5 and 6) (Barak et al., 1999; Hellstrom et al., 1999; Ihle, 2000).

and/or the placenta. The temporal occurrence of the vascular phenotypes seen in the PDGF-B and PDGFR-β knock outs (Fig 9 a) suggests that loss of paracrine/juxtacrine PC-to-EC signaling promotes endothelial hyperplasia, whereas the increased VEGF-A levels may contribute to the progressive vascular derangement that become apparent with increased embryonic age. A hypothetical scenario for pathogenic cause–effect relationships in PDGF-B and PDGFR-β knock outs is outlined in Fig. 9 b.

Lack of PCs Leads to EC Hyperplasia

Based on morphological studies, it has been proposed that PCs control vessel sprouting and branching (Nehls et al., 1992, 1994). Despite the near complete lack of PCs in the PDGF-B and PDGFR-β knock out brains, we show that blood vessels in this tissue have a normal number of branch points and a normal microvessel density. However, blood vessels devoid of PCs exhibit several other defects, such as irregular diameter and increased permeability. Interestingly, mutant blood vessels show EC hyperplasia at time points before any signs of systemic disease. Normally, the first blood vessels sprout into the brain parenchyma around E 10. EC hyperplasia in PDGF-B and PDGFR-β knock outs was evident from E 11.5. At this time, PCs are already present on the wild-type brain blood vessels but are missing in the PDGF-B and PDGFR-β knock outs. The temporal correlation between failure of PCs recruitment and endothelial hyperplasia suggests that the lack of PCs directly regulates EC number. Consistent with this, coculture experiments have suggested that PC–EC contact inhibits both EC and PC proliferation (Antonelli-Orlidge et al., 1989; Hirschi et al., 1999). Morphological studies indicate a negative correlation between the presence of PCs and the proliferation of ECs in experimental and pathological angiogenesis (Cogan et al., 1961; Kuwabara and Cogan, 1963; Crocker et al., 1970; Benjamin et al., 1999).

Pericytic Influence on Capillary Morphogenesis

Although it is plausible that the EC hyperplasia in PDGF-B and PDGFR-β embryos may contribute to an increased capillary diameter, the reduced EC junctional circumference and the increased EC cytoplasmic thickness suggest

that ECs are more crowded in the microvessel wall. An average 25% increase in vessel diameter, as seen in the mutants, would result on average in a two times increase in tension in the vascular wall at constant blood pressure. This could, by itself or in combination with the lack of the structural support from PCs, promote microaneurysm formation. A schematic illustration of the capillary EC phenotype in the PDGF-B/PDGFR-β knock outs is shown in Fig. 10.

The cause of the luminal EC projections seen in the mutants is currently poorly understood. A similar ultrastructural EC phenotype has been described for the fibulin-1 knock out (Kostka, G., and R. Timpl, personal communication). Fibulin-1 is a component of the vascular basement membrane shared between ECs and PCs and could, accordingly, be of importance for the normal EC–PC interaction. During the development of the pecten oculi of the chick eye, there is degeneration and loss of PCs (Gerhardt et al., 2000). This is accompanied by an increase in EC number and the formation of excessive luminal EC projections. Thus, a role for PCs in controlling EC proliferation and morphology is suggested also from a normal developmental process in the chick eye.

Endothelial Hyperplasia Precedes VEGF-A Upregulation

VEGF-A is a potent endothelial mitogen critical for embryogenesis (for review see Ferrara, 1999). A narrow range of VEGF concentration is required for normal cardiovascular development, since a 50% reduction or a two- to threefold increase in VEGF-A expression both lead to embryonic lethality in mice (Carmeliet et al., 1996; Ferrara et al., 1996; Gerber et al., 1999; Miquerol et al., 2000). We found that VEGF-A levels were upregulated more than twofold in PDGF-B and PDGFR-β knock out embryos at late gestation. However, VEGF-A was not significantly upregulated at the earliest time points of EC hyperplasia in mutants but became progressively elevated from E 13.5 on. Although an increased expression of VEGF-A does not seem to explain the EC hyperplasia in the knock outs before E 13.5, VEGF-A may support the hyperplastic state later. In a model of regulated VEGF expression in tumors, Benjamin and co-workers (1999) demonstrated that VEGF withdrawal leads to selective EC apoptosis and degeneration of tumor vessels lacking PC/vSMCs. Their study suggests that either VEGF or contact with PC/vSMCs is sufficient to promote EC survival in tumor vessels. In analogy with their study, the absence of PCs in PDGF-B and PDGFR-β knock out brains may be compensated by increased VEGF-A levels, allowing for survival of the increased number of ECs.

Upregulation of VEGF-A and Other Markers of Metabolic Stress Suggests Systemic Defects in PDGF-B and PDGFR-β Knock Outs

VEGF-A is induced by hypoxia and hypoglycemia both at the RNA and protein levels (Shweiki et al., 1992; Stein et al., 1998). Upregulation of VEGF-A, Glut-1, GRP-78, LDH, and PGK suggests that PDGF-B and PDGFR-β knock out embryos are influenced by metabolic stress. Several causes of hypoxia and/or hypoglycemia in these knock outs can be envisioned. First, it might originate from low tissue oxygenation due to malfunctioning microvessels. Second, the labyrinthine layer of the placenta has a reduced number of PCs and trophoblasts in PDGF-B and PDGFR-β knock outs, which results in dilated embryonic vessels and in a reduced fetal–maternal interface (Ohlsson et al., 1999). This might result in inefficient exchange between the fetal and maternal blood vessels, leading to shortage of oxygen and nutrients and accumulation of waste products in mutant embryos. It is interesting to note that the earliest morphological signs of placenta defects in mutants occur at E 13.5, coincident with the increased VEGF-A levels. Third, the PDGF-B and PDGFR-β knock out hearts are dilated and hypotrophic, which may have systemic consequences (Levéen et al., 1994; Hellstrom et al., 1999). A scenario for the pathogenic cause–effect relationships in PDGF-B and PDGFR-β knock outs is outlined in Fig. 9 b.

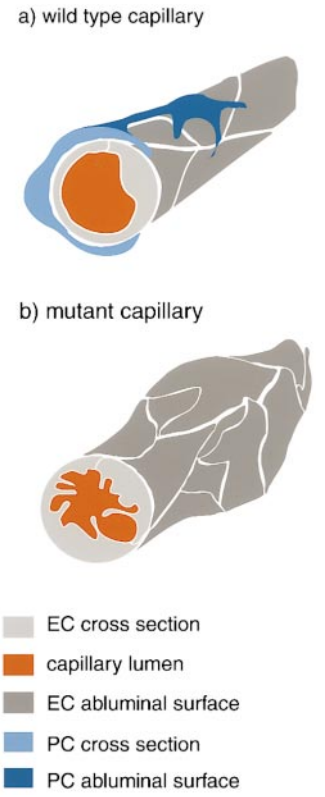

Figure 10. Schematic illustration of wild-type and knock out capillaries based on the combined data of morphological, morphometric, and immunocytochemical analysis. The absence of PCs in the PDGF-B and PDGFR-β knock outs leads to blood vessel dilation, EC hyperplasia, and microaneurysm formation. The ECs exhibit luminal membrane folding and highly variable cytoplasmic thickness and size.

Vascular Leakage Is Accompanied by Elevated Vesiculation and Altered Junctional Architecture

The edema in late PDGF-B and PDGFR-β mutant embryos prompted us to analyze markers of EC junctions and transcellular transport. Vesicular transport by caveolae is a major pathway for transcellular permeability (for review see Feng et al., 1999). The increase in caveolae and caveolin-1 staining seen in PDGF-B and PDGFR-β mutants suggests that this may cause (a portion of) the vascular leakage in these embryos.

Paracellular transport is controlled by tight and adherens junctions. Tight junctions are built up by lipids and transmembrane proteins, which are anchored to the cytoskeleton (for review see Kniesel and Wolburg, 2000).

Freeze fracture analysis of the endothelial tight junctions revealed no differences between the wild type and the PDGF-B knock out. However, the transmembrane protein, occludin, was redistributed and showed less distinct tight junctional staining in the PDGF-B and PDGFR-β knock outs. The series of events leading to the developmental acquisition of blood–brain barrier properties in ECs has been described to involve the shift of occludin from cytoplasmic pools to the tight junctions (Gerhardt et al., 1999). Accordingly, the elevated cytoplasmic and reduced junctional localization of occludin in the knock outs may be interpreted as a sign of less mature tight junctions. Similarly, the adherens junction protein VE-cadherin was partially redistributed from a junctional to a cytoplasmic location. Together, this suggests that tight and adherens junctions are formed in knock outs but do not exhibit the full degree of differentiation. It is known that VEGF-A promotes both paracellular and transcellular permeability in ECs by increasing the number of caveolae and by rearranging occludin and VE-cadherin (Vasile et al., 1999). It is therefore possible that the increased levels of VEGF-A directly induce vascular leakage in the PDGF-B and PDGFR-β knock outs. This idea is strengthened by the fact that there are no differences in caveolin-1, occludin, or VE-cadherin staining at E 12.5, when VEGF-A is not yet upregulated, and no increase in vascular leakage has been observed in the mutants. Furthermore, high expression of VEGF-A has been correlated with leaky blood vessels in several experimental and pathological conditions (for reviews see Dvorak et al., 1999; Ferrara and Alitalo, 1999).

The vascular leakage in the PDGF-B and PDGFR-β knock out brains is likely a major cause of edema and glial swelling. This could be the trigger of the upregulation of the astrocyte-specific water channel aquaporin-4 (Wen et al., 1999) in glial cells surrounding the abnormal blood vessels in PDGF-B and PDGFR-β knock outs, which is consistent with aquaporin-4 upregulation in other conditions where vascular leakage and brain edema is prominent (Vajda et al., 2000).

In summary, our analysis suggests that PCs regulate EC number during embryonic angiogenesis. Elevated VEGF-A levels, possibly secondary to systemic metabolic stress in PDGF-B and PDGFR-β knock outs, may also contribute to the vascular abnormalities seen in these embryos, in particular to the increased vascular leakage observed at late gestation. Our analyses suggest that the pathogenesis of vascular abnormalities also in other mouse mutants is complex and may depend on a combination of local cues, e.g., mechanical properties or signaling events, and secondary systemic influences (Fig. 9 b). The number of mouse knock outs with lethal cardiovascular syndromes available for analysis is steadily increasing, but for most of these, the understanding is still rather poor. The determination of pathogenic chains of events in these mutants is challenging but may also have important implications for the understanding of microvessel disease in humans, such as diabetic microangiopathy.

We thank Dr. Hubert Kalbacher for cooperation in the production of the claudin-5 antibody and Eva-Maria Knittel for excellent technical assistance with the electron microscopic and freeze fracture analysis.

This work was supported by the Swedish Cancer Foundation, The Novo Nordisk Foundation, IngaBritt and Arne Lundberg Foundation, and Göran Gustafsson Foundation (to C. Betsholtz); the Deutsche Forschungsgemeinschaft (grant Wo 215/14-1; to H. Wolburg); the Graduiertenkolleg Neurobiologie of the University of Tuebingen and the European Molecular Biology Organization (to H. Gerhardt); and the Ludwig Institute for Cancer Research (to M. Hellstrom and C. Betsholtz).

Submitted: 21 September 2000
Revised: 26 January 2001
Accepted: 13 March 2001

References

Antonelli-Orlidge, A., K.B. Saunders, S.R. Smith, and P.A. D'Amore. 1989. An activated form of TGF-β is produced by co-cultures of endothelial cells and pericytes. *Proc. Natl. Acad. Sci. USA*. 86:4544–4548.

Barak, Y., M.C. Nelson, E.S. Ong, Y.Z. Jones, P. Ruiz-Lozano, K.R. Chien, A. Koder, and R.M. Evans. 1999. PPAR γ is required for placental, cardiac, and adipose tissue development. *Mol. Cell*. 4:585–595.

Beck, L.J., and P.A. D'Amore. 1997. Vascular development: cellular and molecular regulation. *FASEB J.* 11:365–373.

Benjamin, L., I. Hemo, and E. Keshet. 1998. A plasticity window for blood vessel remodelling is defined by pericyte coverage of the preformed endothelial network and is regulated by PDGF-B and VEGF. *Development*. 125:1591–1598.

Benjamin, L.E., D. Golijanin, A. Itin, D. Pode, and E. Keshet. 1999. Selective ablation of immature blood vessels in established human tumors follows vascular endothelial growth factor withdrawal. *J. Clin. Invest*. 103:159–165.

Breier, G., F. Breviario, L. Caveda, R. Berthier, H. Schnurch, U. Gotsch, D. Vestweber, W. Risau, and E. Dejana. 1996. Molecular cloning and expression of murine vascular endothelial-cadherin in early stage development of cardiovascular system. *Blood*. 87:630–641.

Carmeliet, P., V. Ferreira, G. Breier, S. Pollefeyt, L. Kieckens, M. Gertsenstein, M. Fahrig, A. Vandenhoeck, K. Harpal, C. Eberhardt, et al. 1996. Abnormal blood vessel development and lethality in embryos lacking a single VEGF allele. *Nature*. 380:435–439.

Cogan, D.G., D. Toussaint, and T. Kuwabara. 1961. Retinal vascular patterns. IV. Diabetic retinopathy. *Arch. Ophthalmol.* 66:366–378.

Crocker, D.J., T.M. Murad, and J.C. Geer. 1970. Role of the pericyte in wound healing. An ultrastructural study. *Exp. Mole. Pathol.* 13:51–65.

Crosby, J.R., R.A. Seifert, P. Soriano, and D.F. Bowen-Pope. 1998. Chimaeric analysis reveals role of PDGF receptors in all muscle lineages. *Nat. Genet*. 18:385–388.

Dvorak, H.F., J.A. Nagy, D. Feng, L.F. Brown, and A.M. Dvorak. 1999. Vascular permeability factor/vascular endothelial growth factor and the significance of microvascular hyperpermeability in angiogenesis. *Curr. Top. Microbiol. Immunol*. 237:97–132.

Feng, D., J.A. Nagy, K. Pyne, I. Hammel, H.F. Dvorak, and A.M. Dvorak. 1999. Pathways of macromolecular extravasation across microvascular endothelium in response to VPF/VEGF and other vasoactive mediators. *Microcirculation*. 6:23–44.

Ferrara, N. 1999. Molecular and biological properties of vascular endothelial growth factor. *J. Mol. Med*. 77:527–543.

Ferrara, N., and K. Alitalo. 1999. Clinical applications of angiogenic growth factors and their inhibitors. *Nat. Med*. 5:1359–1364.

Ferrara, N., K. Carver-Moore, H. Chen, M. Dowd, L. Lu, K.S. O'Shea, L. Powell-Braxton, K.J. Hillan, and M.W. Moore. 1996. Heterozygous embryonic lethality induced by targeted inactivation of the VEGF gene. *Nature*. 380: 439–442.

Furuse, M., T. Hirase, M. Itoh, A. Nagafuchi, S. Yonemura, S.A. Tsukita, and S.H. Tsukita. 1993. Occludin: a novel integral membrane protein localizing at tight junctions. *J. Cell Biol.* 123:1777–1788.

Gerber, H.P., K.J. Hillan, A.M. Ryan, J. Kowalski, G.A. Keller, L. Rangell, B.D. Wright, F. Radtke, M. Aguet, and N. Ferrara. 1999. VEGF is required for growth and survival in neonatal mice. *Development*. 126:1149–1159.

Gerhardt, H., S. Liebner, C. Redies, and H. Wolburg. 1999. N-cadherin expression in endothelial cells during early angiogenesis in the eye and brain of the chicken: relation to blood-retina/blood-barrier barrier development. *Eur. J. Neur*. 11:1191–1201.

Gerhardt, H., S. Liebner, and H. Wolfburg. 1996. The pectin oculi of the chicken as a new in vivo model of the blood–brain barrier. *Cell Tissue Res.* 28:91–100.

Gerhardt, H., G. Rascher, J. Schuck, U. Weigold, C. Redies, and H. Wolburg. 2000. R- and B-cadherin expression defines subpopulations of glial cells involved in axonal guidance in the optic nerve head of the chicken. *Glia*. 31: 131–143.

Hellstrom, M., M. Kalen, P. Lindahl, A. Abramsson, and C. Betsholtz. 1999. Role of PDGF-B and PDGFR-β in recruitment of vascular smooth muscle cells and pericytes during embryonic blood vessel formation in the mouse. *Development*. 126:3047–3055.

Hirschi, K.K., S.A. Rohovsky, L.H. Beck, S.R. Smith, and P.A. D'Amore. 1999. Endothelial cells modulate the proliferation of mural cell precursors via platelet-derived growth factor-BB and heterotypic cell contact. *Circ. Res.* 84:

298–305.
Hirschi, K.K., S.A. Rohovsky, and P.A. D'Amore. 1998. PDGF, TGF-β, and heterotypic cell–cell interactions mediate endothelial cell–induced recruitment of 10T1/2 cells and their differentiation to a smooth muscle fate. *J. Cell Biol*. 141:805–814 (erratum published 141:1287).
Holmgren, L., A. Glaser, S. Pfeifer-Ohlsson, and R. Ohlsson. 1991. Angiogenesis during human extraembryonic development involves the spatiotemporal control of PDGF ligand and receptor gene expression. *Development*. 113: 749–754.
Ihle, J.N. 2000. The challenges of translating knockout phenotypes into gene function. *Cell*. 102:131–134.
Kniesel, U., and H. Wolburg. 2000. The tight junctions of the blood-brain barrier. *Cell. Mol. Neurobiol.* 20:57–76.
Kniesel, U., W. Risau, and H. Wolburg. 1996. Development of blood-brain barrier tight junctions in the rat cortex. *Dev. Brain Res.* 96:229–240.
Kuwabara, T., and D.G. Cogan. 1963. Retinal vascular patterns. VI. Mural cells of the retinal capillaries. *Arch. Ophthalmol*. 69:492–502.
Levéen, P., M. Pekny, S. Gebre-Medhin, B. Swolin, E. Larsson, and C. Betsholtz. 1994. Mice deficient for PDGF B show renal, cardiovascular, and hematological abnormalities. *Genes Dev*. 8:1875–1887.
Li, D.Y., L.K. Sorensen, B.S. Brooke, L.D. Urness, E.C. Davis, D.G. Taylor, B.B. Boak, and D.P. Wendel. 1999. Defective angiogenesis in mice lacking endoglin. *Science*. 284:1534–1537.
Liebner, S., A. Fischmann, G. Rascher, F. Duffner, E.H. Grote, H. Kalbacher, and H. Wolburg. 2000. Claudin-1 and claudin-5 expression and tight junction morphology are altered in blood vessels of human glioblastoma multiforme. *Acta Neuropathol*. 100:323–331.
Lindahl, P., B. Johansson, P. Levéen, and C. Betsholtz. 1997. Pericyte loss and microaneurysm formation in PDGF-B-deficient mice. *Science*. 277:242–245.
Lindahl, P., M. Hellstrom, M. Kalen, L. Karlsson, M. Pekny, M. Pekna, P. Soriano, and C. Betsholtz. 1998. Paracrine PDGF-B/PDGF-Rβ signaling controls mesangial cell development in kidney glomeruli. *Development*. 125: 3313–3322.
Miquerol, L., B.L. Langille, and A. Nagy. 2000. Embryonic development is disrupted by modest increases in vascular endothelial growth factor gene expression. *Development*. 127:3941–3946.
Navarro, P., L. Ruco, and E. Dejana. 1998. Differential localization of VE- and N-cadherins in human endothelial cells: VE-cadherin competes with N-cadherin for junctional localization. *J. Cell Biol*. 140:1475–1484.
Nehls, V., K. Denzer, and D. Drenckhahn. 1992. Pericyte involvement in capillary sprouting during angiogenesis in situ. *Cell Tissue Res*. 270:469–474.
Nehls, V., E. Schuchardt, and D. Drenckhahn. 1994. The effect of fibroblasts, vascular smooth muscle cells, and pericytes on sprout formation of endothelial cells in a fibrin gel angiogenesis system. *Microvasc. Res*. 48:349–363.
Nicosia, R.F., and S. Villaschi. 1995. Rat aortic smooth muscle cells become pericytes during angiogenesis in vitro. *Lab. Invest*. 73:658–666.
Oh, S.P., T. Seki, K.A. Goss, T. Imamura, Y. Yi, P.K. Donahoe, L. Li, K. Miyazono, P. ten Dijke, S. Kim, and E. Li. 2000. Activin receptor-like kinase 1 modulates transforming growth factor-β 1 signaling in the regulation of angiogenesis. *Proc. Natl. Acad. Sci. USA*. 97:2626–2631.
Ohlsson, R., P. Falck, M. Hellstrom, P. Lindahl, H. Bostrom, G. Franklin, L. Ahrlund-Richter, J. Pollard, P. Soriano, and C. Betsholtz. 1999. PDGFB regulates the development of the labyrinthine layer of the mouse fetal placenta. *Dev. Biol*. 212:124–136.
Orlidge, A., and P.A. D'Amore. 1987. Inhibition of capillary endothelial cell growth by pericytes and smooth muscle cells. *J. Cell Biol.* 105:1455–1462.
Parton, R.G. 1996. Caveolae and caveolins. *Curr. Opin. Cell Biol*. 8:542–548.
Patan, S. 1998. TIE1 and TIE2 receptor tyrosine kinases inversely regulate embryonic angiogenesis by the mechanism of intussusceptive microvascular growth. *Microvasc. Res*. 56:1–21.
Risau, W. 1997. Mechanisms of angiogenesis. *Nature*. 386:671–674.
Sato, Y., and D.B. Rifkin. 1989. Inhibition of endothelial cell movement by pericytes and smooth muscle cells: activation of a latent transforming growth factor β 1–like molecule by plasmin during co-culture. *J. Cell Biol.* 109:309–315.
Shweiki, D., A. Itin, D. Soffer, and E. Keshet. 1992. Vascular endothelial growth factor induced by hypoxia may mediate hypoxia-initiated angiogenesis. *Nature*. 359:843–845.
Sims, D.E. 1986. The pericyte—a review. *Tissue Cell*. 18:153–174.
Soriano, P. 1994. Abnormal kidney development and hematological disorders in PDGF β-receptor mutant mice. *Genes Dev*. 8:1888–1896.
Stein, I., A. Itin, P. Einat, R. Skaliter, Z. Grossman, and E. Keshet. 1998. Translation of vascular endothelial growth factor mRNA by internal ribosome entry: implications for translation under hypoxia. *Mol. Cell. Biol*. 18:3112–3119.
Suri, C., P.F. Jones, S. Patan, S. Bartunkova, P.C. Maisonpierre, S. Davis, T.N. Sato, and G.D. Yancopolous. 1996. Requisite role of angiopoietin-1, a ligand for the TIE2 receptor, during embryonic development. *Cell*. 87:1171–1180.
Vajda, Z., D. Promeneur, T. Doczi, E. Sulyok, J. Frokiaer, O.P. Ottersen, and S. Nielsen. 2000. Increased aquaporin-4 immunoreactivity in rat brain in response to systemic hyponatremia. *Biochem. Biophys. Res. Commun*. 270: 495–503.
Vasile, E., H. Qu, H.F. Dvorak, and A.M. Dvorak. 1999. Caveolae and vesiculo-vacuolar organelles in bovine capillary endothelial cells cultured with VPF/VEGF on floating Matrigel-collagen gels. *J. Histochem. Cytochem*. 47: 159–167.
Vikkula, M., L.M. Boon, K.L. Carraway III, J.T. Calvert, A.J. Diamonti, B. Goumnerov, K.A. Pasyk, D.A. Marchuk, M.L. Warman, L.C. Cantley, et al. 1996. Vascular Dysmorphogenesis caused by an activating mutation in the receptor tyrosine kinase TIE2. *Cell*. 87:1181–1190.
Wen, H., E.A. Nagelhus, M. Amiry-Moghaddam, P. Agre, O.P. Ottersen, and S. Nielsen. 1999. Ontogeny of water transport in rat brain: postnatal expression of the aquaporin-4 water channel. *Eur. J. Neurosci*. 11:935–945.
Yang, X., L.H. Castilla, X. Xu, C. Li, J. Gotay, M. Weinstein, P.P. Liu, and C.X. Deng. 1999. Angiogenesis defects and mesenchymal apoptosis in mice lacking SMAD5. *Development*. 126:1571–1580.